Cameron J. Ritchie, BSME • J. David Godwin, MD • Carl R. Crawford, PhD • William Stanford, MD
Hirofumi Anno, MD • Yongmin Kim, PhD

Minimum Scan Speeds for Suppression of Motion Artifacts in CT[1]

Cardiac and ventilatory motions cause artifacts at chest computed tomography (CT). To determine how short the scan times on third-generation units must be to avoid such artifacts, motion was measured with fast and ultrafast CT scans. Minimum detectable motion was then determined. The longest scan time that avoided a barely perceptible artifact was calculated by dividing the minimum detectable motion by the peak physiologic velocity. The posterior left ventricular wall moved at a maximum velocity of 52.5 mm/sec, necessitating a scan time of 19.1 msec or less to avoid artifact. Lung vessels near the heart moved at 40.5 mm/sec for a scan time of 24.7 msec or less. During quiet breathing, pulmonary vessels moved at 10.7 mm/sec for a scan time of 93.5 msec or less. The authors conclude that the shortest scan time on third-generation units (0.6 second) cannot prevent all artifacts arising from motion in the chest. Even ultrafast scan times (50 msec) are not short enough to eliminate artifacts on these units. Thus, reduction of motion artifacts will require techniques other than fast scanning.

Index terms: Computed tomography (CT), artifact • Computed tomography (CT), physics • Heart, CT, 50.1211 • Lung, CT, 60.1211

Radiology 1992; 185:37–42

[1] From the Departments of Bioengineering (C.J.R.), Radiology (J.D.G., C.R.C.), and Electrical Engineering (Y.K.), University of Washington, 1959 NE Pacific St, Seattle, WA 98195; GE Medical Systems, Milwaukee (C.R.C.); Department of Radiology, University of Iowa, Iowa City (W.S.); and the Department of Radiology, Fujita Health University, Toyoake-city, Japan (H.A.). From the 1990 RSNA scientific assembly. Received October 1, 1991; revision requested November 22; final revision received May 13, 1992; accepted May 14. Supported in part by GE Medical Systems, Milwaukee, and by the Keck Foundation, Los Angeles. **Address reprint requests to** J.D.G.

PHYSIOLOGIC motion causes artifacts in computed tomography (CT) scans. These artifacts are particularly troublesome in scanning the chest, where their sources are cardiac contractions and breathing. Similar artifacts, caused by intestinal peristalsis, affect abdominal scans (1,2). The artifacts are manifested as black or white streaks, bands, dark spots, loss of resolution, or distortion of anatomy (3–5). Clinically, such artifacts are important not only because they degrade image quality (6) but also because they can sometimes be mistaken for pathologic changes such as bronchiectasis (7).

Theoretically, motion artifacts can be reduced by fast scanning (8), gating (9,10), tube alignment (11), corrective reconstruction (12), or postprocessing of the scan (13,14). Several methods have been proposed to correct scans containing motion, but none has proved clinically useful. Fast scanning (0.05–1.0-second scan times) has been used even though the minimum scan speed needed to prevent artifacts has not been established.

To determine the minimum scan speed for a third-generation scanner, we first measured the velocities of cardiac and respiratory motion from fast and ultrafast CT scans. We then determined the minimum detectable motion, that is, the magnitude of motion that caused a barely perceptible artifact on images obtained with a third-generation scanner, and, by combining these data, we calculated the scan times needed to avoid motion artifacts. Our results indicate that the shortest scan time currently available on third-generation scanners (0.6 second) is not fast enough to prevent motion artifacts. Even ultrafast (50-msec) scan times are not fast enough to eliminate artifacts for third-generation scanners.

MATERIALS AND METHODS

We first analyzed CT scans in six patients and measured cardiac and ventilatory motion by plotting the positions and calculating the velocities of pulmonary vessels and of the left border of the heart. Second, we determined the minimum detectable motion by simulating third-generation CT scanning on a computer and incrementally increasing the motion in each scan until our criterion for the existence of an artifact was exceeded. We verified these determinations by scanning a moving phantom. Finally, we calculated the minimum scan speed (expressed as scan times) necessary to avoid artifacts from cardiac and ventilatory motions by dividing the minimum detectable motion by the greatest observed physiologic velocities.

Measurement of Cardiac and Ventilatory Motion

Cardiac motion was analyzed from Imatron C-100 ultrafast CT scans (Imatron, South San Francisco) in three patients. Collimation was 8 mm. For two patients, three levels through the heart were scanned, and, for one patient, four levels were scanned. At each level, 10 (two patients) or eight (one patient) 50-msec scans were acquired with 8-msec interscan delays. Thus, scanning extended over 456 or 572 msec, and scan acquisition, triggered by the R wave of the electrocardiogram, began with end diastole.

Ventilatory motion was analyzed from data acquired on a Toshiba TCT-900S scanner (Toshiba Medical Systems, Tokyo). Three patients underwent scanning with 5-mm collimation, 25° cranial gantry angulation, 120 kVp, and 200 mA. A set of 23 scans was made from 12 seconds of continuous gantry rotation (1 second per rotation) at one anatomic level while the patient exhaled from full inspiration to full expiration (the vital capacity) over 10 seconds. Each scan was reconstructed from 240° of angular information (acquired in 0.6 second), and one scan was obtained every 0.5 second.

Abbreviation: FWTM = full-width-at-tenth-maximum.

For both cardiac and ventilatory motion analysis, videotaped images of the CT scans were digitized and then analyzed with an image processing program (Optimas; BioScan, Edmonds, Wash). (Videotaped images were used because the image processing program was designed to read video frames.) From the cardiac data, four sets of scans were selected on the basis of how clearly the anatomy of interest was depicted, and seven lung vessels close to the heart wall and 10 heart wall positions on the left side were analyzed. From the ventilatory data, seven vessels far from the heart wall (to eliminate the effect of cardiac motion) were selected for analysis. The spatial coordinates of the structures of interest (the cardiac wall and lung vessels) were determined from the digitized images, and these positions were plotted. (Coordinates of lung vessels were taken at the center of the mass of the vessel.)

To establish a single point on the left ventricular wall to track for motion analysis, a ray was derived that was perpendicular to the contour of the free wall of the ventricle and that extended from the center of the mass of the heart, as seen on the two-dimensional CT scan. Cardiac motion was determined from plots of the coordinates of the intersection of this ray with the heart wall on each of the eight or 10 frames of each run of the Imatron data.

Because expiration was prolonged to 10 seconds with the Toshiba data and the expiratory volume was the entire vital capacity, we scaled the ventilatory position data to simulate normal quiet breathing, as might occur if a patient (eg, unconscious) were unable to comply with instructions to hold his breath. We estimated that the vital capacity was 4,000 mL, whereas, in a normal breathing cycle, the tidal volume would be 500 mL (15). In the respiratory maneuver used in scanning, exhalation occurred over 10 seconds, whereas, in quiet breathing, a respiratory cycle would last about 4 seconds (15), one-third of which would be accounted for by inhalation and two-thirds by exhalation. The resulting scale factor was calculated to be 0.937. To represent the worst possible case for respiratory motion, that is, the maximum rate of expiration that would occur during forced exhalation, we also scaled the ventilatory position data as if the patient were able to exhale the entire 4,000 mL at the rate at which a normal person could exhale during the 1st second of forced expiration. (The volume exhaled in the 1st second of forced expiration is normally 80% of the vital capacity.) The resulting scaling factor was 12.5.

The position plots were used to calculate velocities. Velocities were calculated by dividing the distances between the positions of the object on successive scans in the series by the time between scans.

Determination of Minimum Detectable Motion

Computer simulations of CT scanning of a moving object were used to determine the magnitude of motion that would cause a barely perceptible artifact. The computer program simulated a third-generation CT scanner with the following parameters: 630-mm source to isocenter distance; 1,100-mm source to detector distance; 25.4-mm-high detectors on 1-mm centers, with an active width of 0.8 mm, 9.2° fan angle (yielding a 200-mm field of view); 800 projections; 351 samples per projection; and 360° of projection data. The simulated test object was a 10 × 10 × 100-mm ellipsoid of attenuation equal to that of water (0 HU) scanned in cross section and surrounded by air (−1,000 HU).

Ramp-filtered, back-projected images with 0.78-mm pixels were generated in the simulations (equivalent to scanning a 40-cm field of view and reconstructing a 512 × 512-pixel image with a GE 9800 unit [GE Medical Systems, Milwaukee]). Ramp filtering was used because it approximates the bone algorithm on the GE 9800 unit that we and others (16) use for reconstructing chest CT scans. To simulate the effect of noise in obscuring small amounts of motion, we determined the mean and the standard deviation of the noise resulting from scanning air with an actual GE 9800 unit (120 kVp, 40 mA), generated a corresponding image of noise with a Gaussian distribution, and added the noise image to the images of the test object (17).

Different patterns of motion of the test object were programmed, varying in magnitude, phase (with respect to the angular position of the gantry), frequency, and type of motion. The simulated motion began with the start of scanning, and the initial direction of the center ray of the x-ray fan was vertical. For the computation of minimum scan speed, we used horizontal, linear motion of constant velocity. This motion was selected, first, because it is similar to clinically observed motion and, second, because motion along the horizontal axis is the most likely to cause motion artifact.

For each simulation, we first generated a static image, that is, an image with the object at rest. We then generated a series of nine motion images in which the magnitude of motion was incremented by 0.1 mm per image through a maximum of 1.0 mm. For each motion image, a series of profiles of the test object was made at every 5°, and the full-width-at-tenth-maximum (FWTM) of each profile of the test object was calculated. FWTM was calculated as the width in pixels of a profile through the image at one-tenth the maximum pixel value. At each angle, the FWTM of the motion image was compared with the FWTM at the corresponding angle of the static image of each of the nine motion images. When the difference between any one of the radial set of FWTMs was greater than the size of 1 pixel (0.78 mm), the distortion of the object was just perceptible, and minimum detectable motion was deemed to have occurred.

To validate the accuracy of our computer programs in simulating a real third-generation CT scanner, we scanned a 10-mm-diameter acrylic peg, surrounded by air, with a GE 9800 unit while the peg was driven by a computer-controlled motor that could be programmed for motion in three dimensions, with a resolution of 0.025 mm (18). Two-second scans were obtained at 40 mA and 120 kVp, with 10-mm collimation, and were reconstructed with a 40-cm field of view. We programmed the motion phantom to recreate the horizontal motion of the test object in the computer simulations and then scanned the peg as the magnitude of motion increased from 0.0 to 1.0 mm in 0.1-mm increments. We then performed an identical FWTM analysis, as was done on the simulation images.

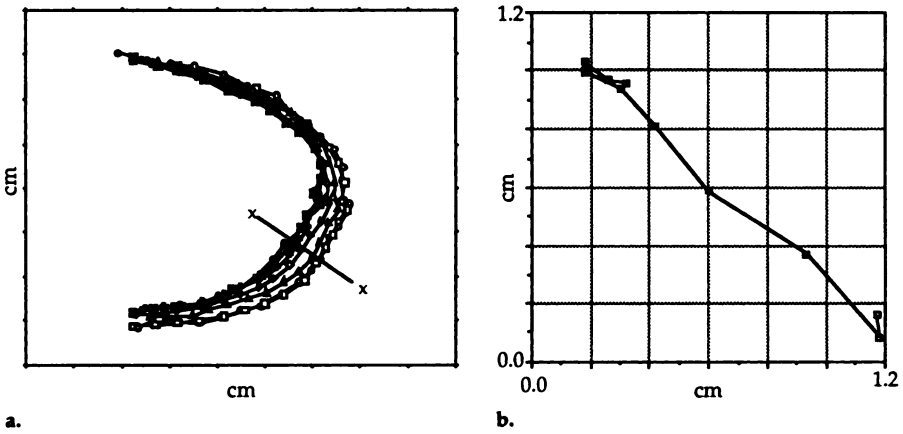

Figure 1. Left ventricular wall motion. **(a)** Graph shows several heart wall contours. Ten contours were generated from 10 50-msec images. The interscan delay was 8 msec. Only seven contours are shown for clarity. **(b)** Graph shows a magnification of the heart wall motion along line *x* in **a**. Note the change of direction at end systole.

RESULTS

Characterization of Physiologic Motion

The maximum excursion of the left ventricular wall was along an oblique ray about 30° below the horizontal

Table 1
Velocities of the Heart Wall

Patient No.	Level	Frames Acquired	Velocity (mm/sec)*		
			Maximum	Minimum	Mean
1	Upper	8	49.5	4.4	18.4
1	Middle	8	53.4	11.4	26.4
1	Middle	8	53.2	11.3	29.0
2	Middle	10	49.4	0.4	12.7
2	Middle	10	65.9	2.8	31.3
2	Middle	10	23.2	7.7	16.1
3	Middle	10	47.8	3.0	21.9
3	Middle	10	68.1	5.7	31.5
3	Middle	10	62.7	4.6	22.3
3	Lower	10	52.1	5.4	29.4

* Average velocities were 52.5, 5.7, and 23.9; standard deviations were 12.6, 3.6, and 6.7.

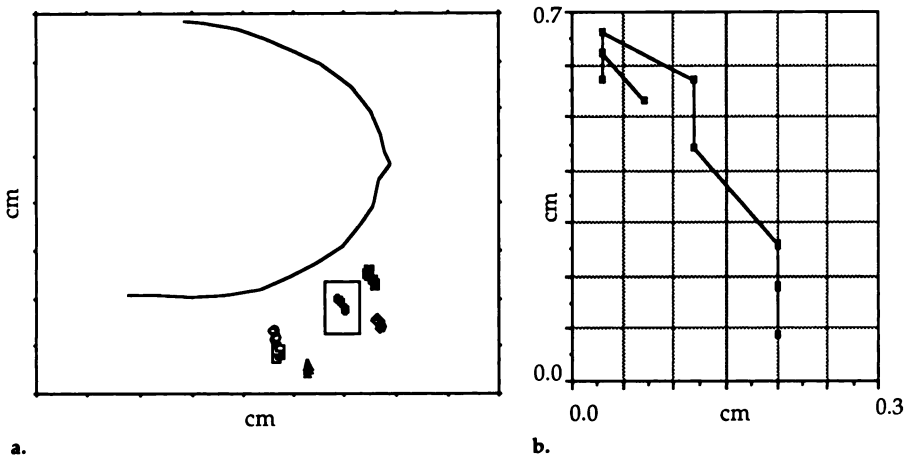

Figure 2. Pulmonary vessel motions resulting from heartbeat. Motions of pulmonary vessels primarily moving due to motion of the left ventricular wall. **(a)** Plot shows the left ventricular wall for reference and the patterns of motion for five vessels. The scale is identical to that in Figure 1a. Data come from 10 50-msec scans with an 8-msec interscan delay. **(b)** Graph shows a magnification of the boxed vessel in **a**, demonstrating motion through end systole and early diastole.

(Fig 1). Maximum velocities ranged from 23.2 to 68.1 mm/sec, with an average of 52.5 mm/sec (Table 1). Lung vessels propelled by cardiac motion moved radially with left ventricular wall motion (Fig 2). Maximum velocities ranged from 31.2 to 68.4 mm/sec, with an average of 40.5 mm/sec (Table 2). Lung vessels moved by respiration demonstrated predominantly anteroposterior motion in the upper chest and radial motion in the lower chest (Fig 3). Maximum velocities scaled for quiet breathing ranged from 6.1 to 20.1 mm/sec, with an average of 10.7 mm/sec; maximum velocities scaled for forced exhalation ranged from 76.1 to 250.6 mm/sec, with an average of 133.4 mm/sec for the approximation of forced exhalation (Table 3).

Velocity varied sinusoidally through the cardiac cycle for the heart wall (Fig 4a) and adjacent lung vessels (Fig 4b). Velocity also varied sinusoidally for lung vessels propelled by respiratory motion (Fig 4c). Maximum velocities of the heart wall and of vessels close to it were similar (Tables 1, 2), whereas the maximum velocities of vessels that were farther from the heart and, therefore, moving primarily because of quiet respiration were lower by a factor of five (Table 3). Vessels moving due to forced exhalation moved at velocities about two and one-half times greater than those of the left ventricular wall.

Minimum Detectable Motion

Minimum detectable motion for horizontal, linear motion from the computer simulations was 1.0 mm. The scan with air yielded a mean of −994 HU and a standard deviation of 1.2 HU. Adding a noise scan based on these figures to the simulated motion images did not alter the calculated minimum detectable motion.

Minimum detectable motion for horizontal motion from the motion phantom was 0.8 mm, in close agreement with the computer simulations. This concordance validates the computer simulations of CT scanning for the analysis of motion artifacts.

Minimum Scan Speed

Minimum scan speed (expressed as scan time) necessary to eliminate artifacts from motion with average maximum cardiac velocity was 19.1 msec (Table 4). The speed necessary to eliminate artifacts caused by quiet breathing was 93.5 msec (Table 4). These values were obtained by dividing the minimum detectable motion from the simulations (1.0 mm) by the physiologic velocities in Tables 1–3.

DISCUSSION

Estimating the magnitude of physiologic motion is the first step in reducing or eliminating motion artifacts. A pilot study such as this is not intended to be exhaustive; we confined our analysis to available CT scans, all of which were obtained for reasons other than analysis of physiologic motion. Furthermore, because the technique for measuring motion is laborious, we examined only a small number of patients, and we cannot determine how great the population variance of velocities would be in a larger series. Also, we did not seek patients with heart or lung disease that might cause extreme values of motion.

However, our results for cardiac motion are confirmed by ultrasonographic determinations of heart wall velocity. Kraunz and Kennedy (19) found the average maximum posterior wall velocity in 25 patients to be 41 mm/sec, corresponding to our result of 52.5 mm/sec. Similarly, Smithen et al (20) found the average maximum velocity in 11 patients to be 37 mm/sec. Velocity data from ventriculograms demonstrated average velocities of the posterior wall of the left ventricle to be 27.8 mm/sec (Sheehan F, unpublished data, 1991). Despite this high degree of concordance, it should be remembered that ultrasonographic, ventriculographic, and CT determinations are not precisely comparable, since the former two measure endocardial motion and the latter measures epicardial motion.

We are not aware of any previous determination of the respiratory excursion of lung vessels in the transverse plane. Although Weiss et al (21)

examined the respiratory excursion of the liver, these determinations apply to longitudinal, not transverse, motion. It is clear, however, that longitudinal motion of lung vessels affected our results. Because lung vessels near the diaphragm cross the scan plane obliquely, some of their longitudinal motion appeared as transverse motion in the scan plane.

The determination of minimum detectable motion clearly depends on how motion artifact is defined. We sought an objective criterion that corresponded to visible changes in the images. We found that a recognizable distortion of the test object corresponded to a 1-pixel difference at FWTM, so we adopted this difference as the objective criterion for determining the presence of motion artifact. We originally considered, but later discarded, the criterion of a 1-pixel difference at full-width-at-half-maximum because we found it to be insensitive to degrees of motion that were clearly visible to the eye.

We also considered using streaking as the criterion for presence of motion artifact but rejected it for two reasons. First, we found that extremely small amounts of motion (approaching the resolution of the motion phantom) generated streaks when the image was viewed with a narrow window; however, at usual window settings (window, 1,000 HU; level, −700 HU), we found that a 1-pixel blur was apparent before streaking became visible, and, thus, the 1-pixel blur was a more sensitive criterion. Second, there are other causes of streaks beside motion (eg, aliasing) so that there are always some streaks at edges even if there is no motion in the object being scanned. Therefore, using streaking as a criterion for motion artifact necessitates detecting a change in streaking, which is subjective and hard to quantify.

Another consideration affecting minimum detectable motion is scanner geometry. A given motion may generate a different artifact depending on scanner geometry, and we have not explored the relative sensitivities of different geometries to motion. Thus, we emphasize that our results apply only to conventional third-generation geometry.

A third consideration affecting minimum detectable motion is the position of the object being scanned. We computed the minimum detectable motion only for the center of the image. Because resolution decreases away from the center of the CT scan, minimum detectable motion would be expected to be greater near the edges of the scan (22,23). Therefore, sensitivity to motion artifacts would also decrease away from the center.

Our finding that scan times exceeding 19.1 msec will not eliminate artifacts caused by observed physiologic motion near the heart is in accord with the conclusions of Ritman et al (24,25), who estimated that scan times of less than 10 msec are necessary to scan the left ventricular wall. Boyd and Lipton (26) concluded from gated cardiac CT studies that 75-msec scans were not adequate to resolve systolic cardiac motion and estimated that scan times of 30–50 msec would be necessary. Furthermore, even for lung structures at some distance from the heart, scan times must be less than 93.5 msec if the patient's breathing cannot be restrained. It is clear from these values that commercially available third-generation scanners with scan times of 0.6–1.0 second will not eliminate motion artifacts. Even if it could operate at ultrafast speed (50 msec), a current third-generation scanner would be unable to prevent cardiac motion artifacts. However, it is not clear how sensitive the fourth-generation 50-msec Imatron C-100

Table 2
Velocities of Pulmonary Vessels Moving Due to Cardiac Motion

Patient No.	Region	Level	Frames Acquired	Velocity (mm/sec)*		
				Maximum	Minimum	Mean
1	Left	Middle	8	68.4	7.6	21.4
1	Left	Middle	8	37.8	7.6	22.9
1	Left	Middle	8	33.8	10.7	19.1
1	Left	Middle	8	37.8	10.7	23.8
3	Left	Middle	10	31.2	0.0	14.6
3	Left	Middle	10	33.8	0.0	18.1
3	Left	Middle	10	40.7	7.6	19.0

* Average velocities were 40.5, 6.3, and 19.9; standard deviations were 12.7, 4.5, and 3.2.

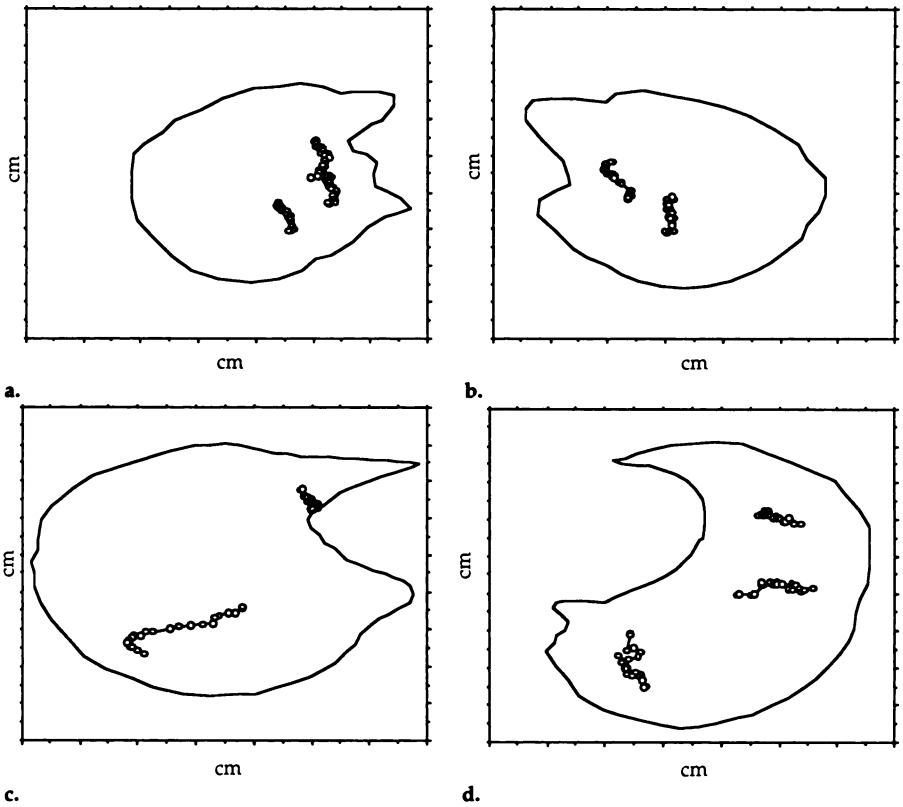

Figure 3. Graphs show lung vessel motions in the right upper lung **(a)**, the left upper lung **(b)**, the right midlung **(c)**, and the left midlung **(d)**. All motions were due to respiration. Outlines of the inner chest wall at full inspiration are also shown for reference. The scale in all four images is constant and equal to that in Figures 1a and 2a. Data come from 12 seconds of continuous scanning, reconstructed into 23 0.5-second images.

Table 3
Velocities of Pulmonary Vessels Moving Due to Respiration

Patient No.	Region	Level	Frames Acquired	Quiet Breathing (mm/sec)*			Forced Exhalation (mm/sec)†		
				Maximum	Minimum	Mean	Maximum	Minimum	Mean
4	Left	Upper	23	8.9	0.0	2.4	111.3	0.0	30.5
4	Left	Upper	23	7.6	0.0	2.3	94.9	0.0	29.3
4	Right	Upper	23	6.7	0.0	2.9	83.2	0.0	36.3
5	Left	Middle	23	6.1	0.0	2.0	76.1	0.0	24.6
6	Left	Lower	23	14.1	0.0	4.8	176.9	0.0	59.7
6	Left	Lower	23	11.2	1.1	4.6	140.6	14.1	57.4
6	Left	Lower	23	20.1	0.0	3.7	250.6	0.0	45.7

* Average velocities were 10.7, 0.2, and 3.3; standard deviations were 5.0, 0.5, and 1.1.
† Average velocities were 133.4, 2.0, and 40.6; standard deviations were 62.5, 5.3, and 14.1.

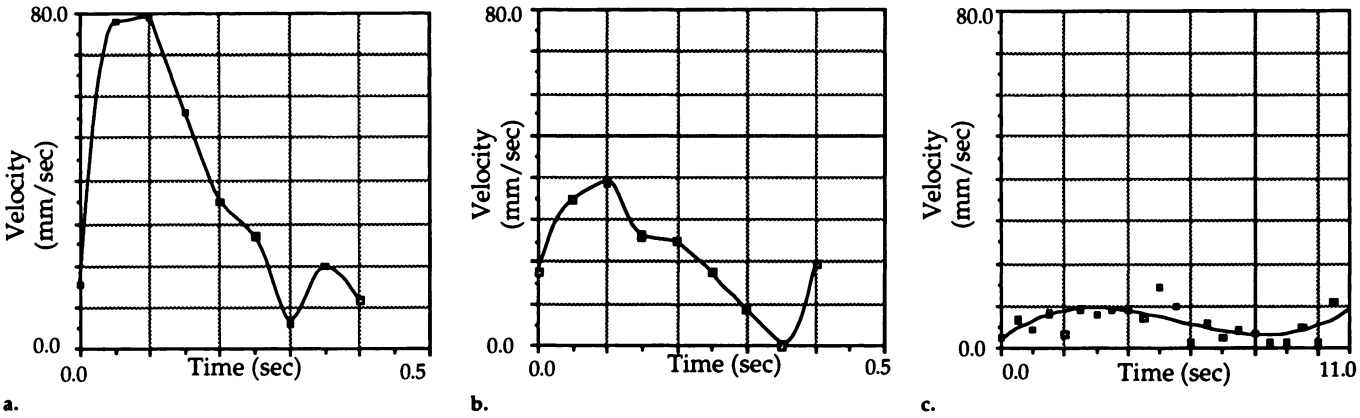

Figure 4. Graphs show velocity versus time of the left ventricular wall moving (**a**), velocity versus time of a vessel moving due to heartbeat (**b**), and velocity versus time of a vessel moving due to respiration (**c**). Note the dampening effect of the lung tissue by comparing the maximum value in **c** to the maximum value in **b**. Calculations were made from the heart wall data in Figure 1b for **a**, from the data in Figure 2b for **b**, and from the data in Figure 3c for **c**.

Table 4
Minimum Scan Speeds

Moving Structure	Average Mean Velocity (msec)	Average Maximum Velocity (msec)
Heart wall	41.8	19.1
Lung vessels (cardiac motion)	50.3	24.7
Lung vessels		
Quiet breathing	303.0	93.5
Forced exhalation	24.6	7.5

scanner is to motion, given its unique geometry.

Approaches other than fast scanning are needed to reduce artifacts in third-generation units. Several alternatives might be considered. From the computer simulations, it is apparent that the scanner is least sensitive to motion along the direction of the center ray of the x-ray fan, and it is most sensitive to motion perpendicular to the direction of the center ray (27). Therefore, if physiologic motion could be predicted, it might be possible to adjust start time and start angle of the gantry to align the x-ray beam to minimize sensitivity to motion.

Another alternative would be to use prospective cardiac gating to acquire most of the scan data during the quiescent period of the cardiac cycle (diastole). For scan times of 500 msec or longer, this approach would have to be supplemented by another technique because the scan time would remain longer than diastole and, therefore, systole would occur late in the scan. A possible supplemental technique would be to anticipate the timing of the next systole and position the gantry at the start of scanning to have the x-ray beam aligned along the axis of the systolic motion. This alignment would ensure that the scan was as insensitive as possible to the unavoidable ventricular motion.

A final alternative would be to implement a more sophisticated corrective reconstruction technique that utilizes models of physiologic motion. Theoretically, knowing the pattern, magnitude, and frequency of motion in advance would allow the use of an algorithm that could remove the motion from the projection data and then reconstruct a motion-free or at least a motion-reduced image (12). ■

Acknowledgments: Florence Sheehan, MD, provided valuable angiographic data on heart wall motion. Robert G. Gould, ScD, assisted in the interpretation of our results.

References

1. Silverman PM, Godwin JD, Moore AV. Technical aspects. In: Godwin JD, ed. Computed tomography of the chest. Hagerstown, Md: Lippincott 1984; 12–16.
2. Stanley RJ. Liver and biliary tract. In: Lee JKT, Sagel SS, Stanley RJ, eds. Computed body tomography. New York: Raven, 1983; 172–174.
3. Scott RL, Payne S, Pinstein ML. Fluid-level motion artifact in computed tomography. J Can Assoc Radiol 1983; 34:294–295.
4. Mayo JR, Müller NL, Henkelman RM. The double-fissure sign: a motion artifact on thin-section CT scans. Radiology 1987; 165:580–581.
5. Kuhns LR, Borlaza G. The twinkling star sign: an aid in differentiating pulmonary vessels from pulmonary nodules on computed tomograms. Radiology 1980; 135: 763–764.
6. Alfidi RJ, MacIntyre WJ, Haaga JR. The effects of biological motion on CT resolution. AJR 1976; 127:11–15.
7. Tarver RD, Conces DJ, Godwin JD. Mo-

tion artifacts on CT simulate bronchiectasis. AJR 1988; 151:1117–1119.
8. Goldberg HI, Gould RG, Feuerstein IM, Sigeti JS, Lipton MJ. Evaluation of ultrafast CT scanning of the adult abdomen. Invest Radiol 1989; 24:537–543.
9. Moore SC, Judy PF. Cardiac computed tomography using redundant-ray prospective gating. Med Phys 1987; 14:193–196.
10. Moore SC, Judy PF, Garnic JD, et al. Prospectively gated cardiac computed tomography. Med Phys 1983; 10:846–855.
11. Crawford CR, Pelc NJ. Method for reducing motion induced image artifacts in projection imaging. U.S. patent 4,994,965, 1991.
12. Crawford CR, King KF, Ritchie CJ, Godwin JD. Respiratory compensation in projection imaging (abstr). Radiology 1990; 177(P):277.
13. Helenon O, Chanin DS, Laval-Jeantet M, Frija J. Artifacts on lung CT scans: removal with Fourier filtration. Radiology 1989; 171:572–574.
14. Yang CK, Orphanoudakis SC, Strohbehn JW. A simulation study of motion artefacts in computed tomography. Phys Med Biol 1982; 27:51–61.
15. West JB. Respiratory physiology: the essentials. 3rd ed. Baltimore: Williams & Wilkins, 1985; 12–17.
16. Zwirewich CV, Terriff B, Müller NL. High-spatial-frequency (bone) algorithm improves quality of standard CT of the thorax. AJR 1989; 153:1169–1173.
17. Box GEP, Muller ME. A note on the generation of random normal deviates. Ann Math Stats 1958; 29:610–611.
18. Ritchie CJ, Peterson E, Yee D, Kim Y, Godwin JD, Crawford CR. A 3-d motion control system for simulation of CT motion artifacts. Proc IEEE EMBS 1989; 11:487–488.
19. Kraunz RF, Kennedy JW. Ultrasonic determination of left ventricular wall motion in normal man: studies at rest and after exercise. Am Heart J 1970; 79:36–43.
20. Smithen CS, Wharton CFP, Sowton E. Independent effects of heart rate and exercise on left ventricular wall movement measured by reflected ultrasound. Am J Cardiol 1972; 30:43–47.
21. Weiss PH, Baker JM, Potchen EJ. Assessment of hepatic respiratory excursion. J Nucl Med 1972; 13:758–759.
22. Crawford CR, Pelc NJ. Angular integration and inter-projection correlation effects in CT reconstructions. Proc IEEE EMBS 1987; 9:1670–1671.
23. Schwierz G, Lichtenberg W, Fuhrer K. Influence of the focal spot on CT image quality. Electromedica 1980; 4:134–139.
24. Ritman EL, Kinsey JH, Robb RA, Harris LD, Gilbert BK. Physics and technical considerations in the design of the DSR: a high temporal resolution volume scanner. AJR 1980; 134:369–374.
25. Ritman EL, Harris LD, Kinsey JH, Robb RA. Computed tomographic imaging of the heart: the dynamic spatial reconstructor. Radiol Clin North Am 1980; 18:547–556.
26. Boyd DP, Lipton MJ. Cardiac computed tomography. Proc IEEE Nucl Sci 1983; 71: 298–307.
27. Crawford CR, Godwin JD, Pelc NJ. Reduction of motion artifacts in computed tomography. Proc IEEE EMBS 1989; 11: 485–486.